NMR IMAGING

Field gradient in one direction

PRINCIPLE OF THE TECHNIQUE

Signal location **- Resonance frequencies of nuclei in the direction of magnetic field gradient g_z:**

$$\nu = \frac{\gamma}{2\pi}(B_0 + gz)$$

Spectrum without and with magnetic field gradient:

Classical NMR

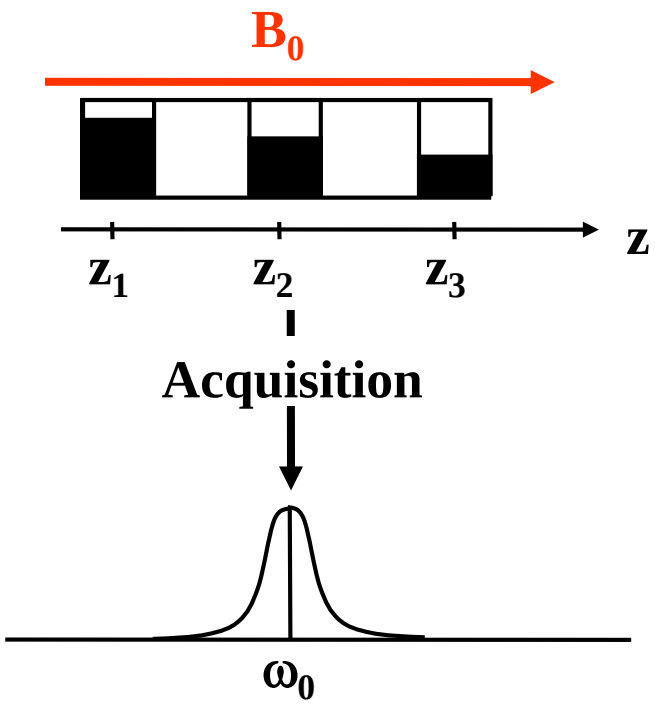

NMR imaging

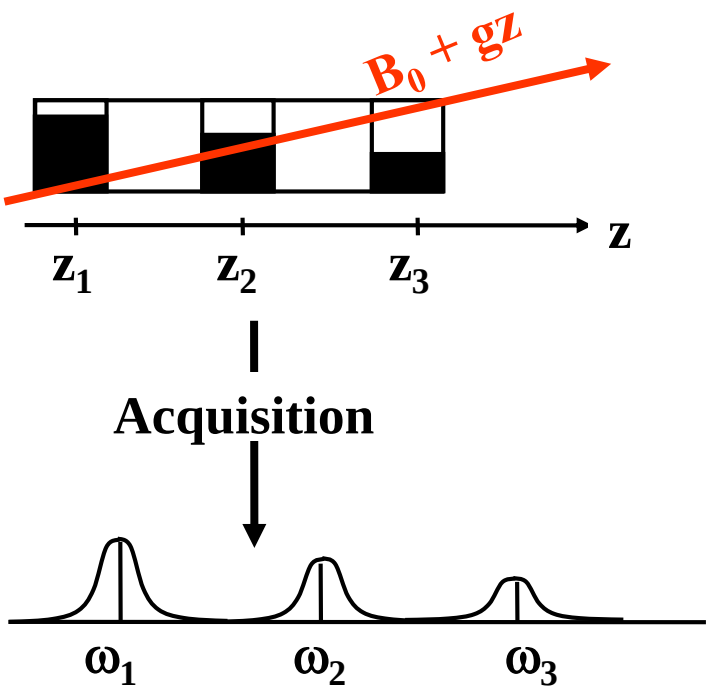

STUDY OF DIFFUSION BY ^{1}H-NMR IMAGING

PRINCIPLE OF THE TECHNIQUE

Signal location **- Resonance frequencies of nuclei in the direction of magnetic field gradient g_z:**

$$\nu = \frac{\gamma}{2\pi}(B_0 + gz)$$

Spectrum without and with magnetic field gradient:

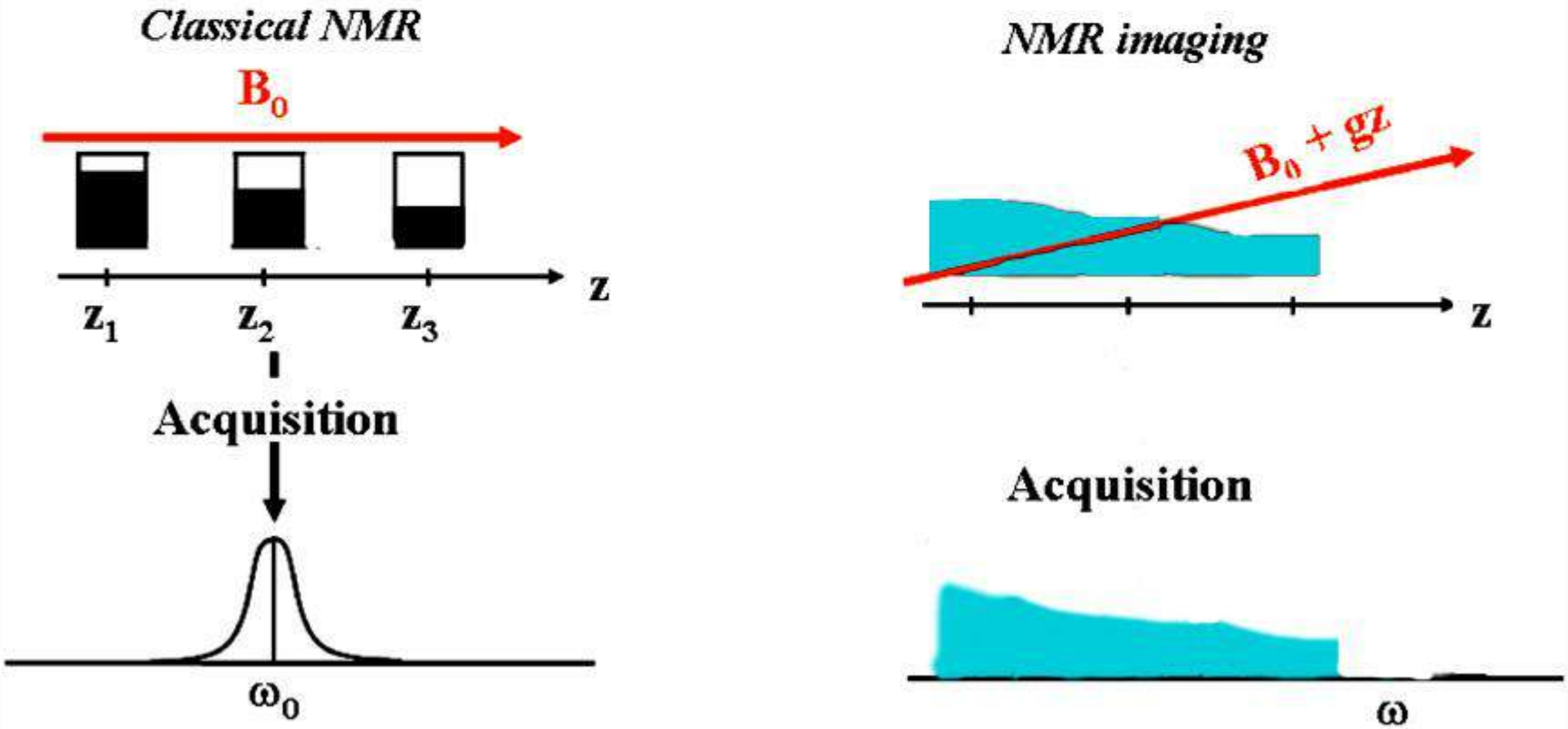

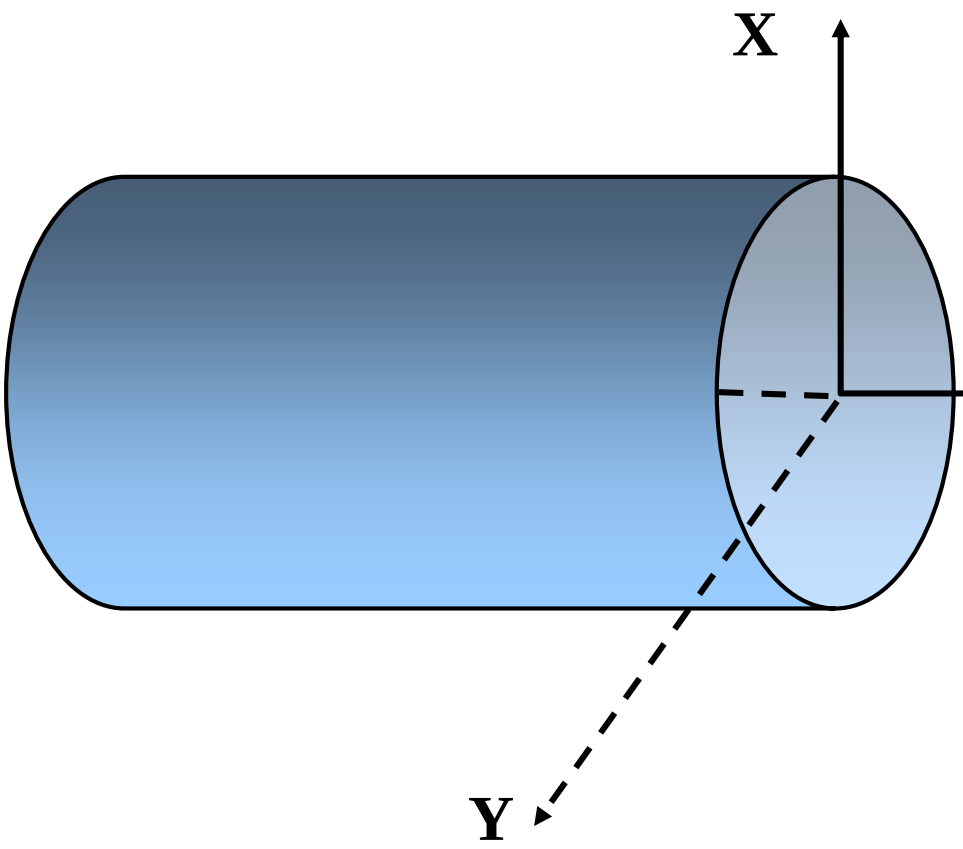

$$Bz = B_0\,(0) + g_0\,Z$$

Gradient

Detected signal :

$$S(\tau) = \sum_{i=1}^{N} \rho_i \exp[i\,\gamma\,g_0\,Z_i\tau].\exp[-\tau/T_2]$$

Adsorption

Adsorption

Diffusion

MODEL OF DIFFUSION

the whole diffusion process can be reduced to :

- **Diffusion in the macropores**
  (intercrystalline diffusion)
  Characteristic length : ℓ
  Diffusion coefficient : D_{inter}
  Characteristic time : τ_{inter}
  K : adsorption equibrium constant
  ε_{inter} : macroporosity

$$\tau_{inter} = \frac{\ell^2 (1 - \varepsilon_{inter}) K}{3\, \varepsilon_{inter}\, D_{inter}}$$

- **Diffusion in the micropores**
  (intracrystalline diffusion)
  Characteristic length : R
  Diffusion coefficient : D_{intra}
  Characteristic time : τ_{intra}

$$\tau_{intra} = \frac{R^2}{15\, D_{intra}}$$

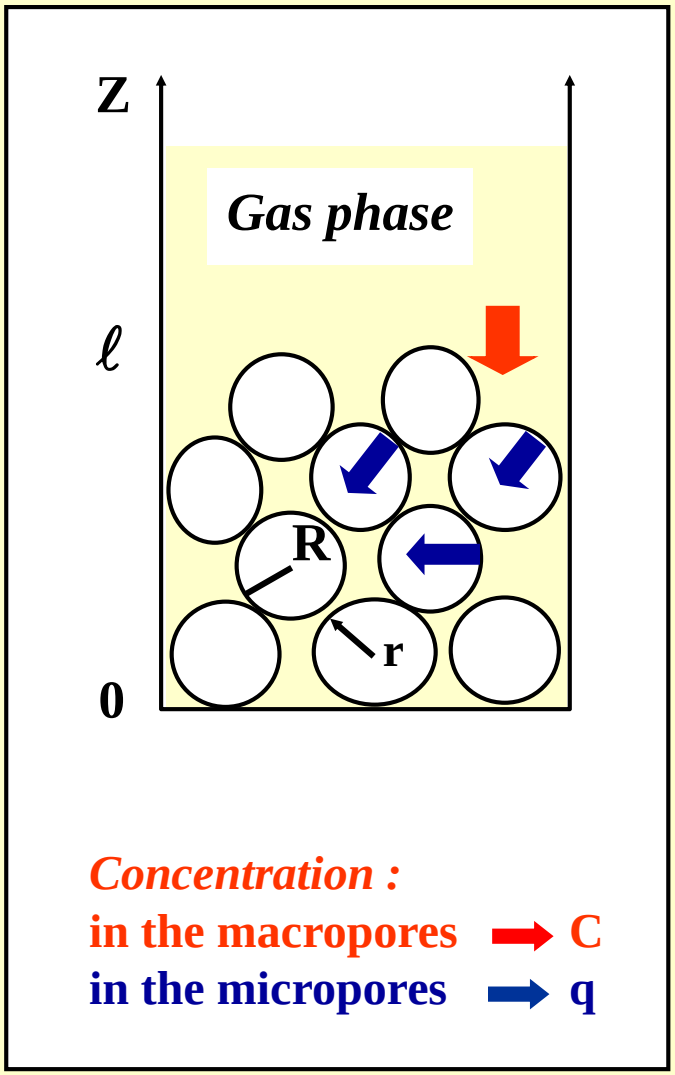

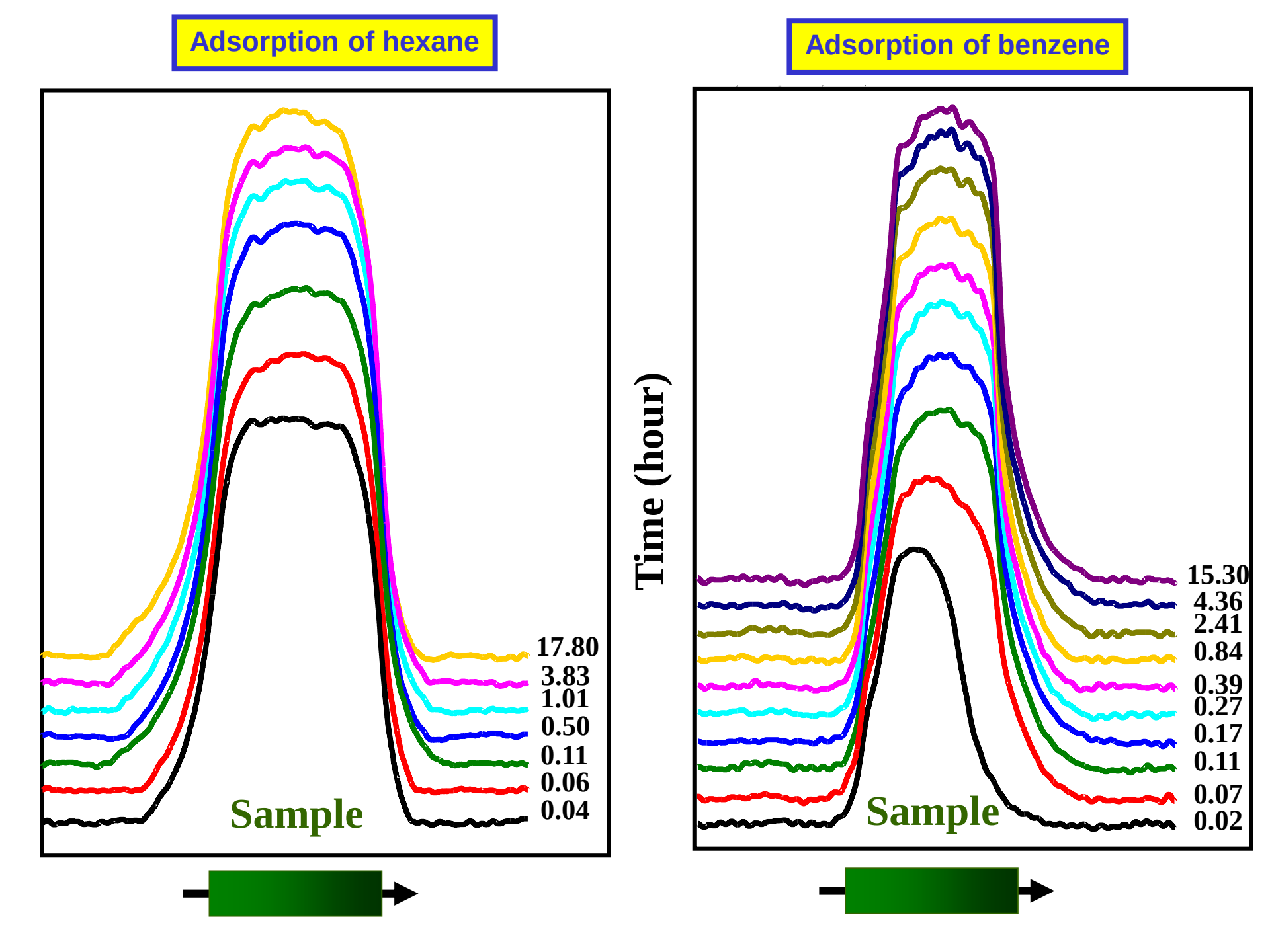
Adsorption of hexane
17.80
3.83
1.01
0.50
0.11
0.06
0.04
Sample
Time (hour)
Adsorption of benzene
15.30
4.36
2.41
0.84
0.39
0.27
0.17
0.11
0.07
0.02
Sample

Competitive Adsorption

Competitive adsorption of hexane and benzene

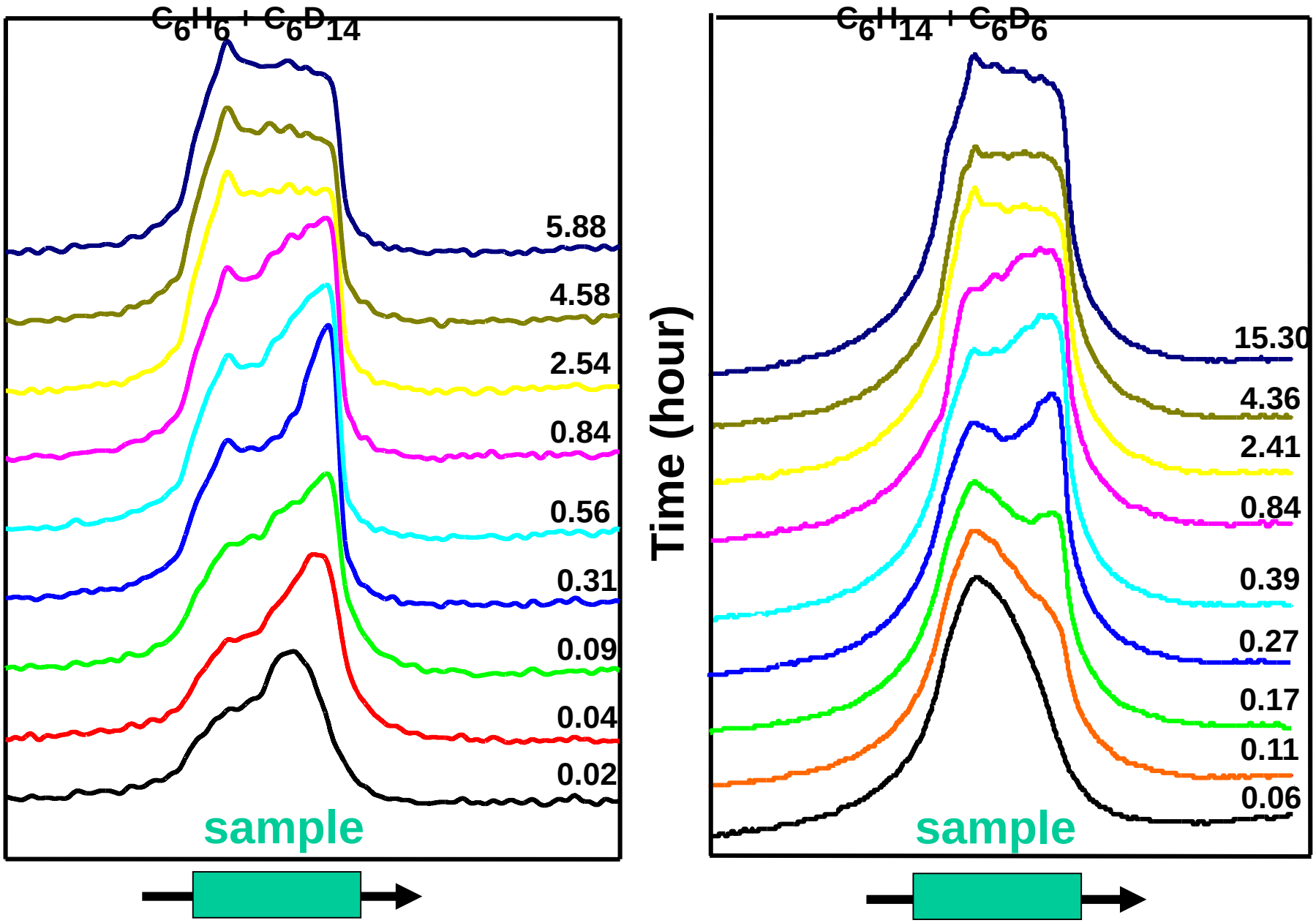

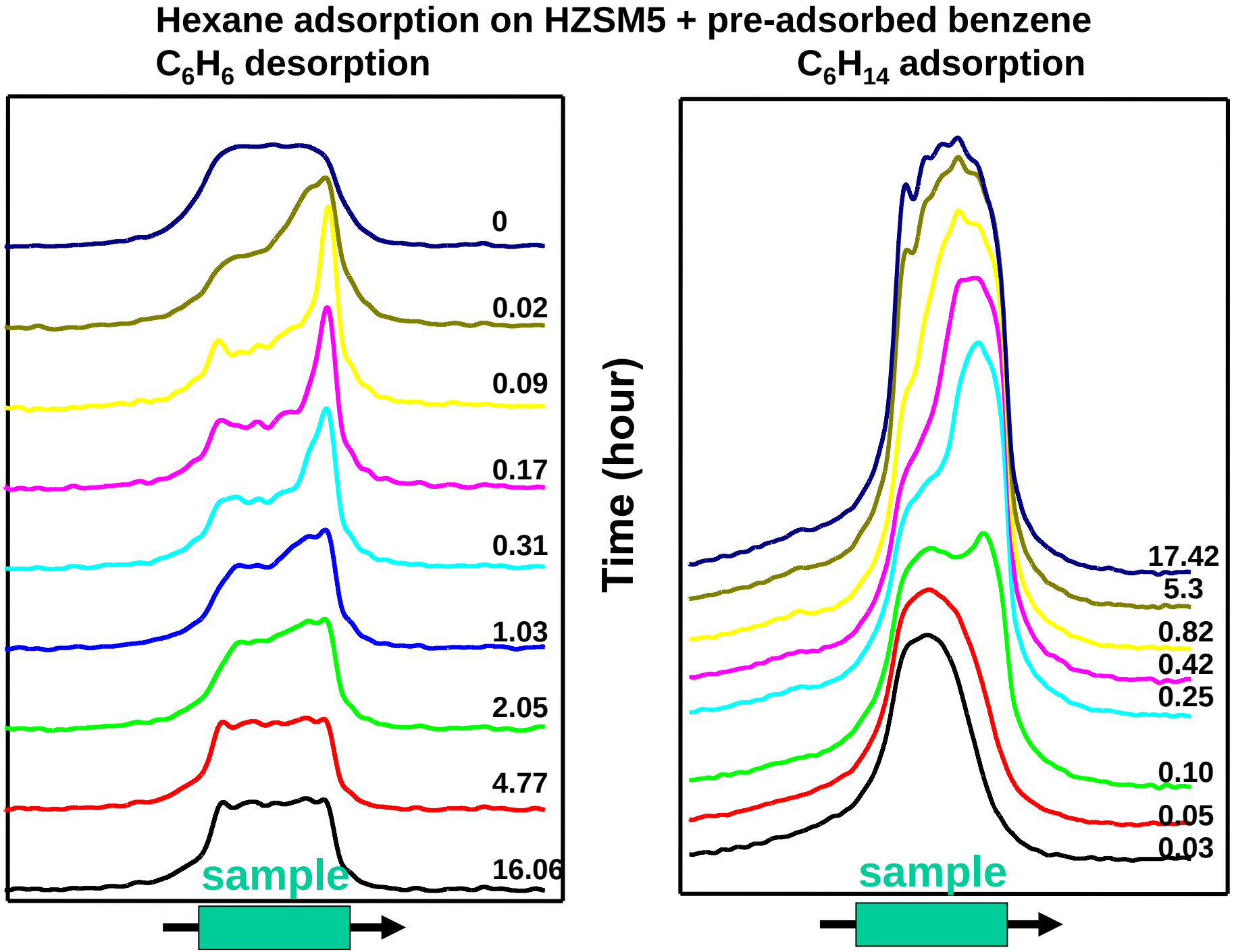
Hexane adsorption on HZSM5 + pre-adsorbed benzene
C6H6 desorption
C6H14 adsorption
Time (hour)
0
0.02
0.09
0.17
0.31
1.03
2.05
4.77
16.06
sample
17.42
5.3
0.82
0.42
0.25
0.10
0.05
0.03
sample

Adsorption of C_6H_{14} and of C_6H_{14}+C_6D_6

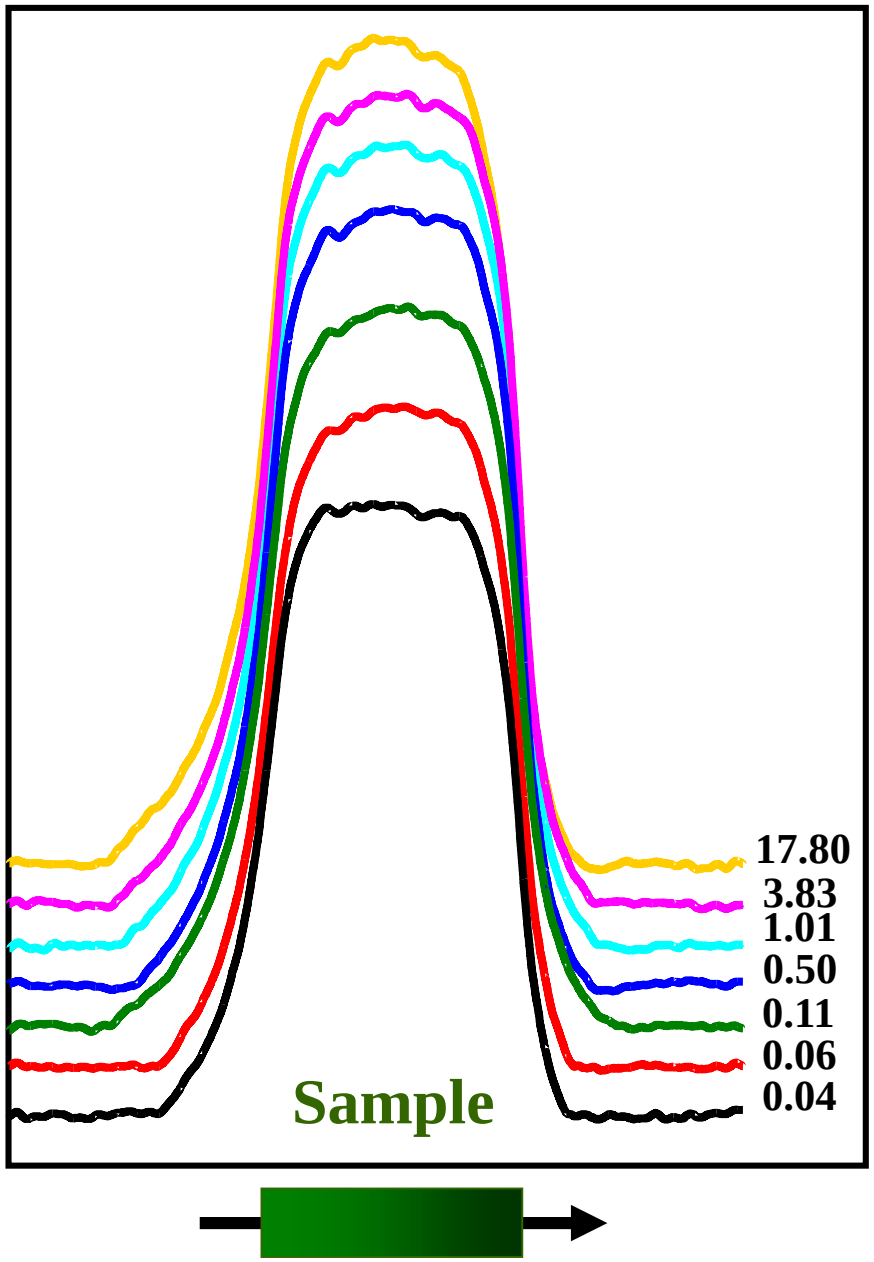

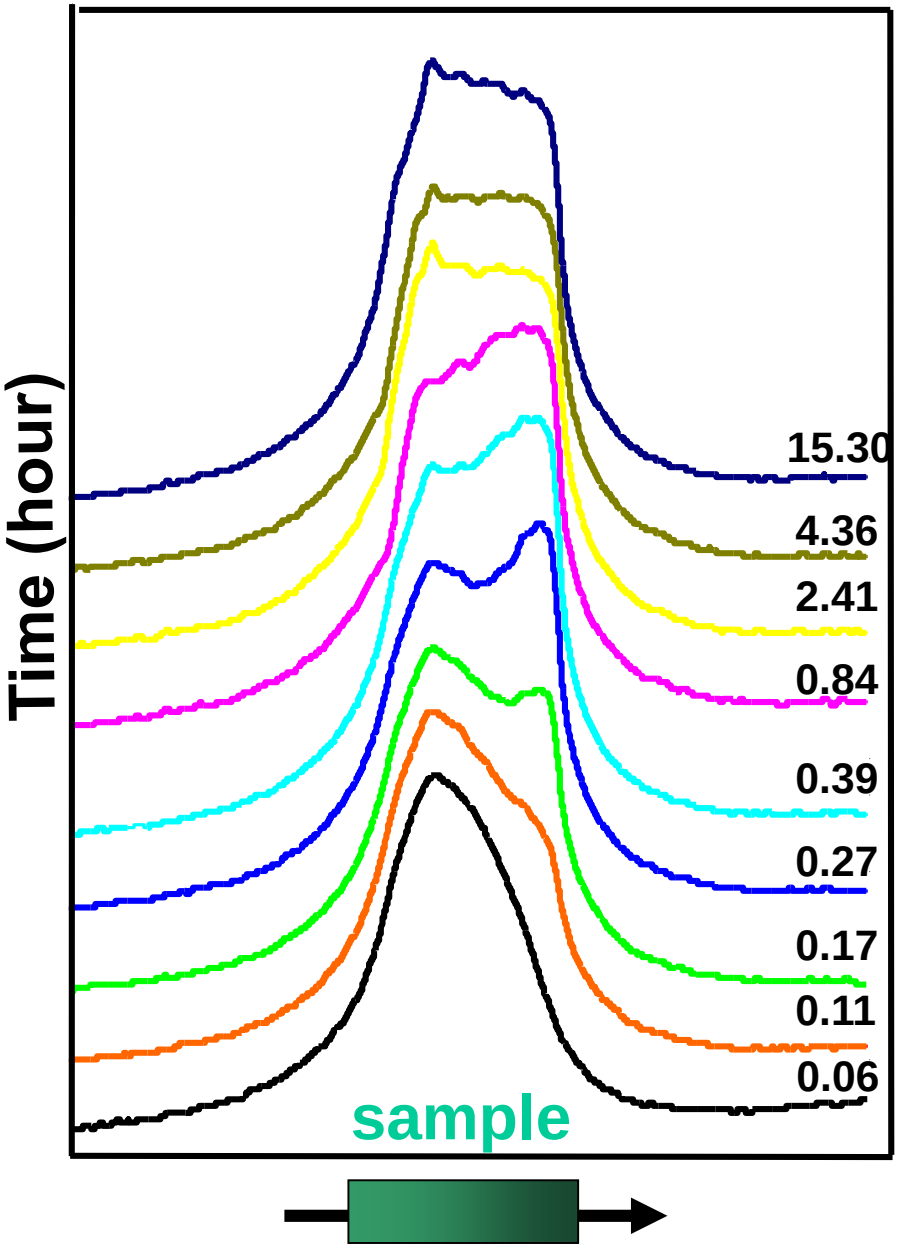

Adsorption of C_6H_6 and of C_6H_6+C_6D_{14}

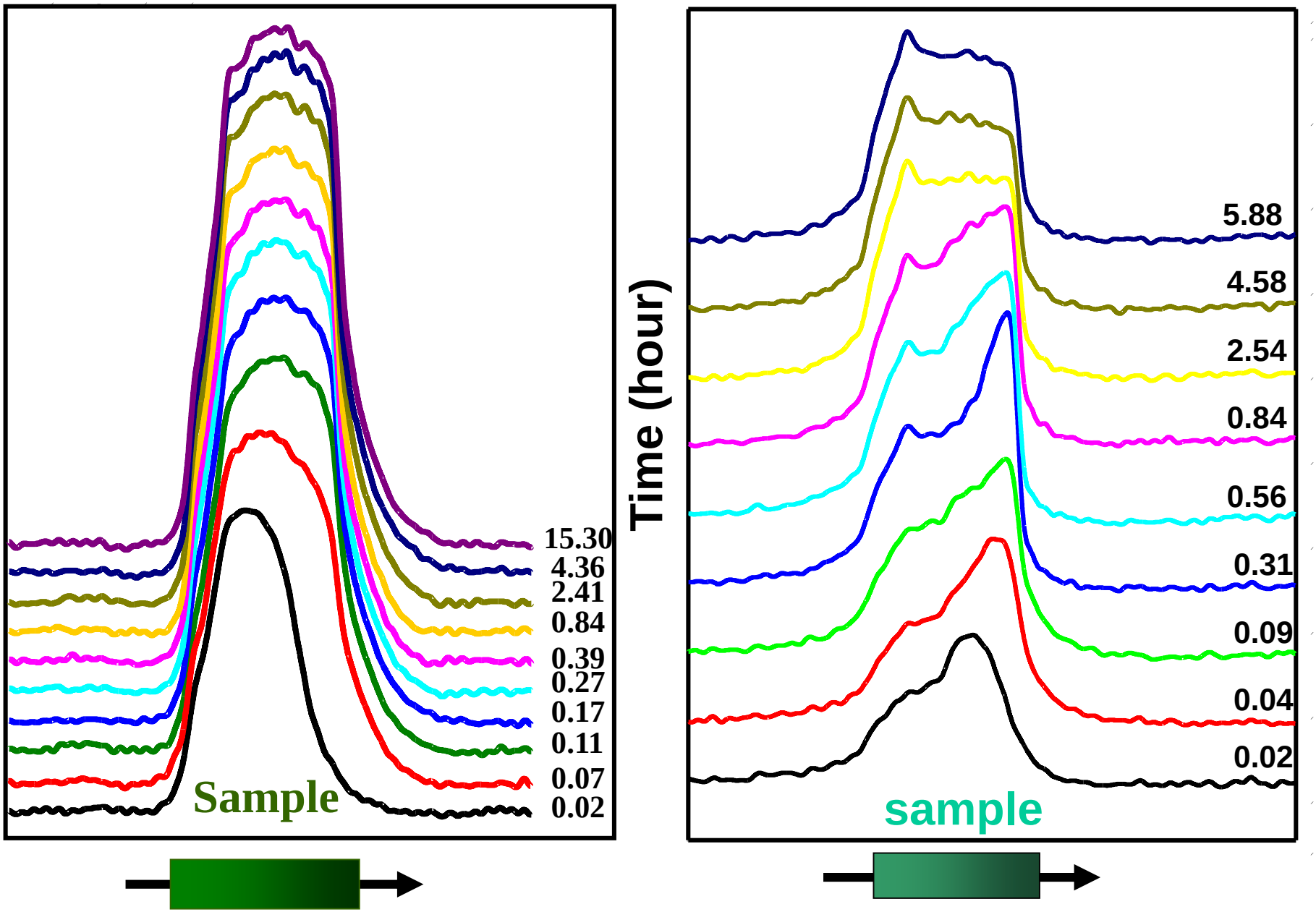

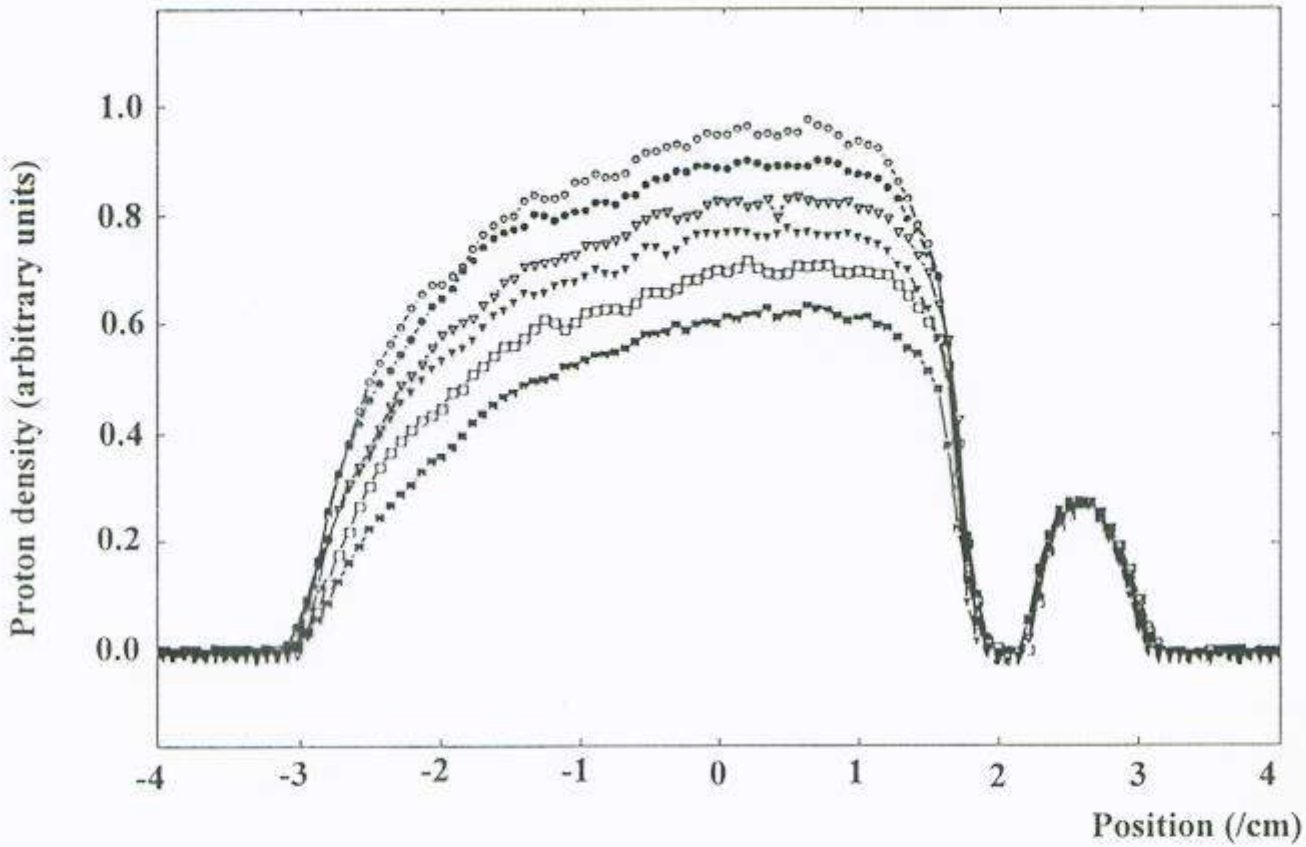

Changes in moisture content along the cement-paste cylinder axis as a function of drying time. SPI profiles, t_p = 290 μs, were acquired at days ❍ 1, ● 3, ▽ 8, ▼ 15, □ 25 and ■ 26. Water migration occurs from the open face (left side) due to a mix of capillary flow and diffusion. The Mn (II) calibration standard is found on the right of the image (+ 2.6 cm).

Field gradient in two directions: Solids

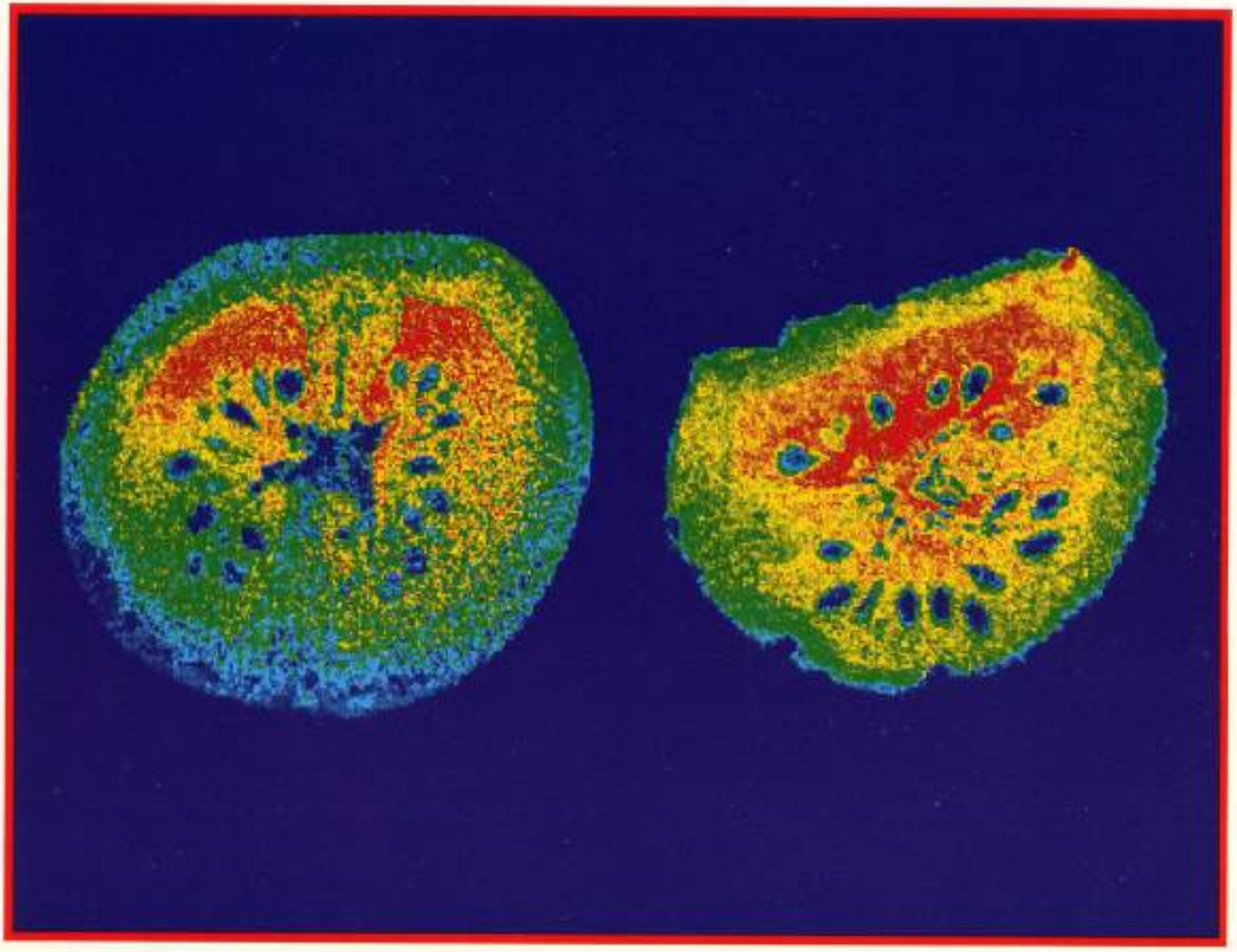

Proton image of a fresh tomato

Image of an "aged" tomato that was dropped once

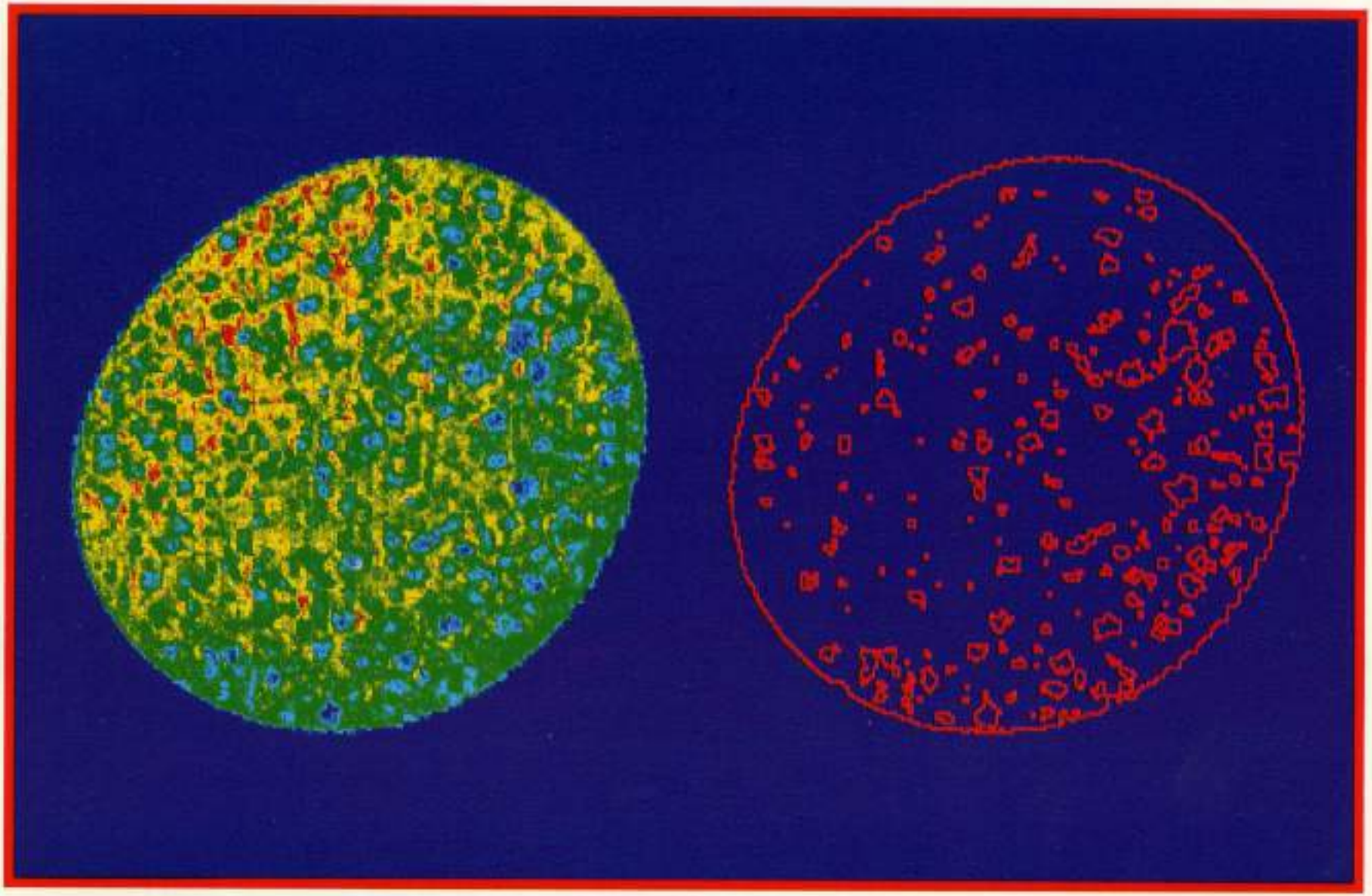

Image of water filled polyurathene foam.

Contour plot of the image showing size and distribution of pores.

The diffusion of methanol into poly(methyl methacrylate) (PMMA) spheres has been studied. The image of a 30 mm PMMA sphere intially submerged in methanol is shown on the left side in the figure below: The images shows the bulk methanol as red areas. The blue circle surrounded by the methanol is the PMMA sphere and shows no methanol intrusion. After 48 hours exposure to the methanol at 30°C, the sphere absorbs a considerable amount of methanol as indicated by the green areas inside the sphere on the right side of the figure.

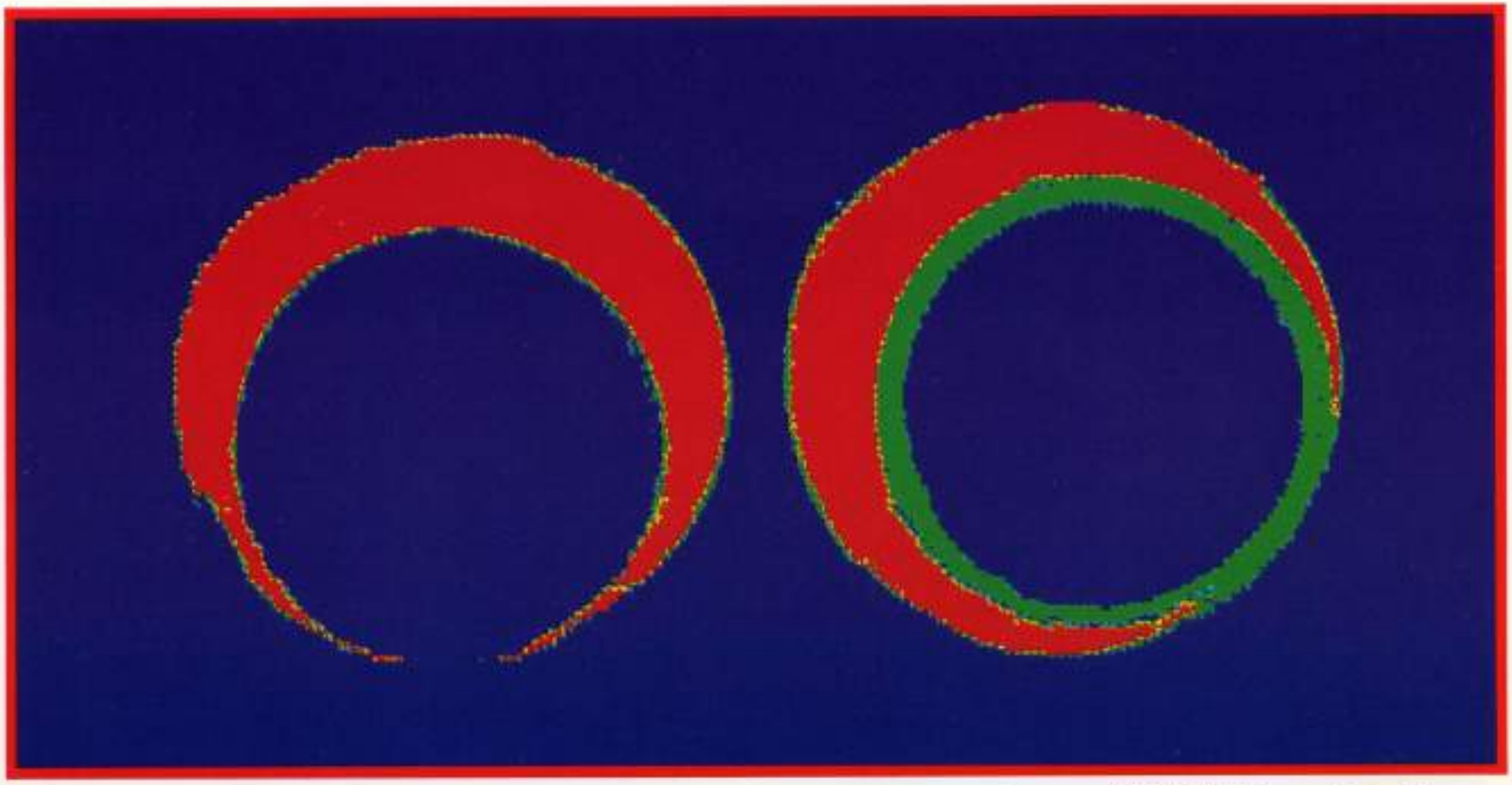

Image of PMMA in methanol, initial submersion.

Image of PMMA in methanol, 48 hours later.

An example of detecting internal defects using NMR imaging is shown in the Figure below which shows the images of pultruded nylon rods reinforced with glass fibers. Two images are shown taken through the same pultruded rod but 0.5 cm apart. The rod was soaked in water and the light areas in the image represent void areas filled with water. The marker in the upper left hand portion of the image is 1 mm in diameter. Comparison of the size of the voids in the pultruded rod indicates that some of the voids approach this magnitude in size.

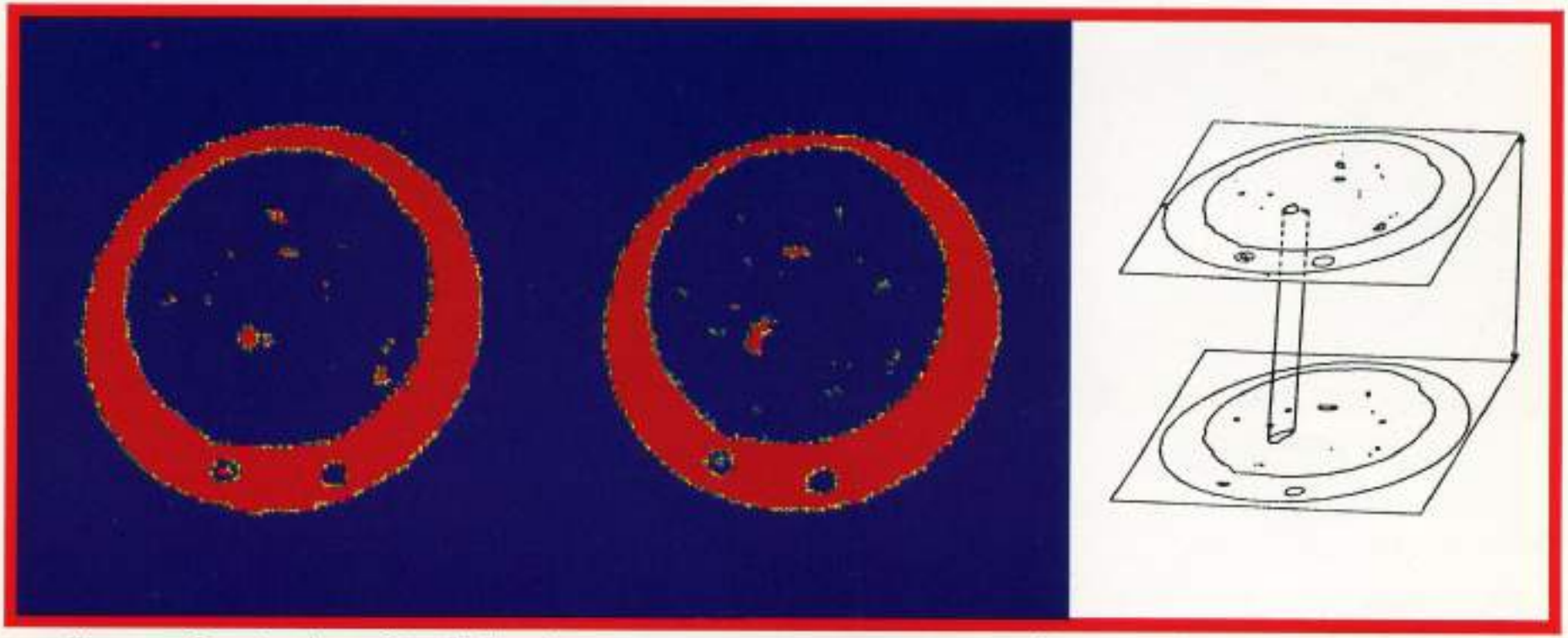

Image of water in pultruded nylon rods reinforced with glass fibers.

Contour plot of image showing presence of tubular void.

Glass fibers are used to impart stiffness to polymeric composites. These glass fibers are often chemically treated at the surface in order to promote adhesion and to improve the hydrothermal stability of the resulting composites. The figure below shows the proton images of two glass-fiber reinforced epoxy composite rods of 2 mm in diameter which have been soaked in water. The glass fibers are approximately 10 μm in diameter. The red areas reflect high concentrations of water where a high level of structural disorder exists. The image on the left shows the rod filled with fibers coated with a coupling agent which prevented good adhesion while the image on the right is with fibers coated with a coupling agent that promoted adhesion.

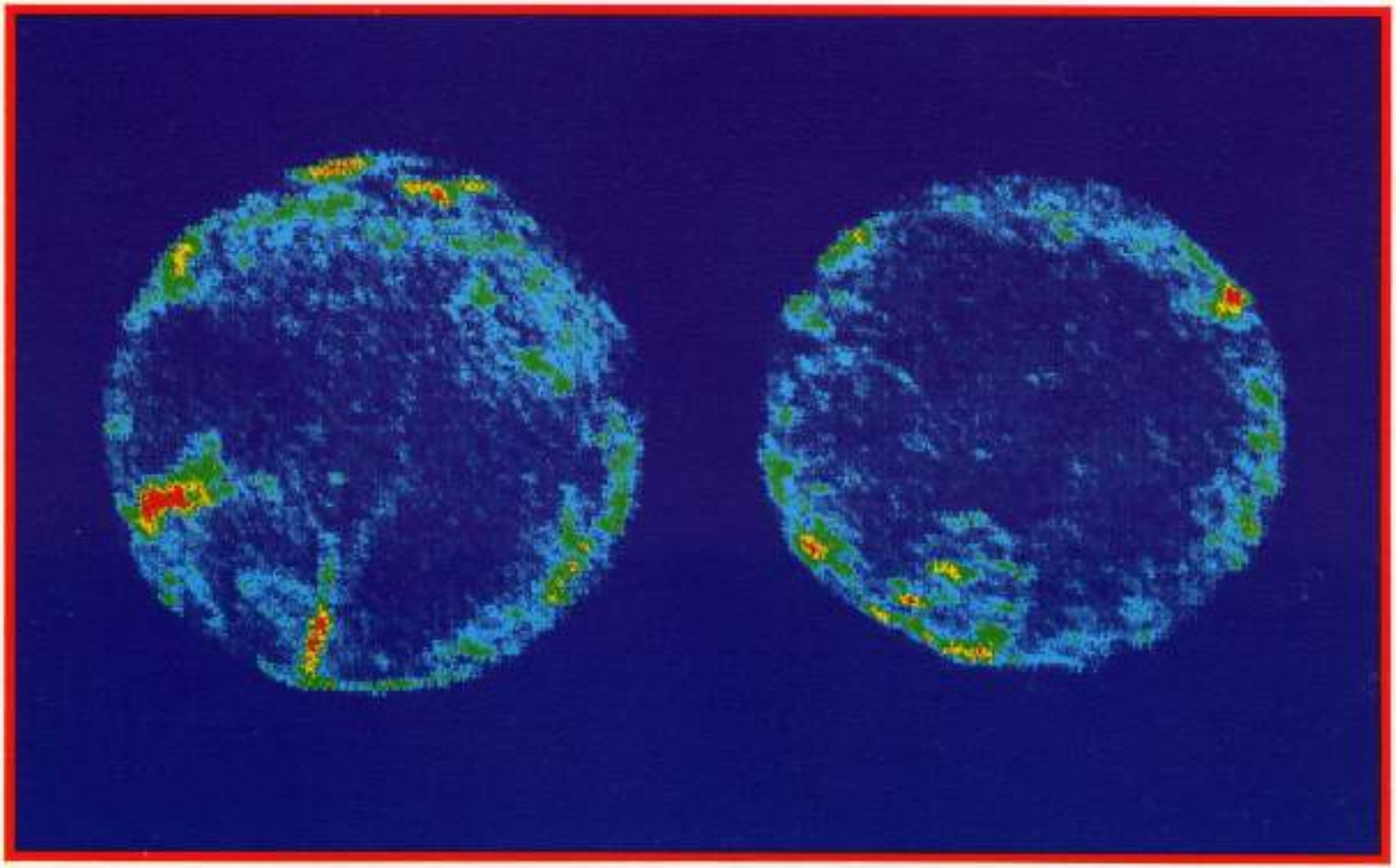

The image below of a predominately natural rubber tubing of 7 mm diameter was obtained using the spin-echo sequence with a echo time of 5 ms. The slice thickness was 5mm and the resolution was 200 μm.

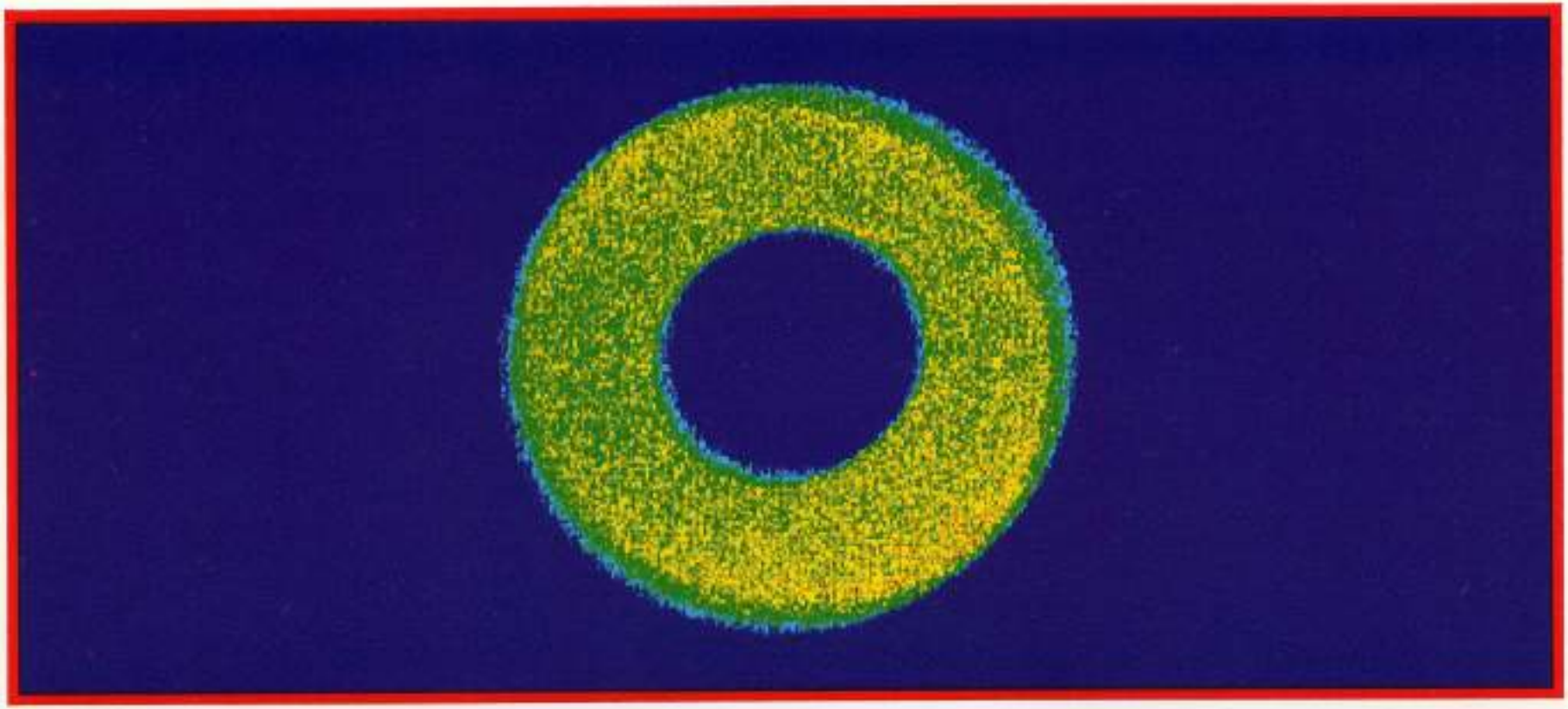

CONCLUSIONS:

The image of the rubber tubing shows that the sample is uniform at least to the resolution limits of the image (200 μm).

The Figure below shows the dioxane proton image using a spin echo pulse sequence of a highly crosslinked sulfur-vulcanized rubber sample which has been swollen in dioxane for 16 days. The top row from left to right shows images with echo times of 30 and 70 ms, followed by a computer generated T2 image. The bottom row shows three-level contour plots of the images in the top row. These contour plots indicate that there is a dioxane background, an intermediate level of dioxane, indicating an intermediate level of crosslinking, and regions of little dioxane which are indicative of a high level of crosslinking.

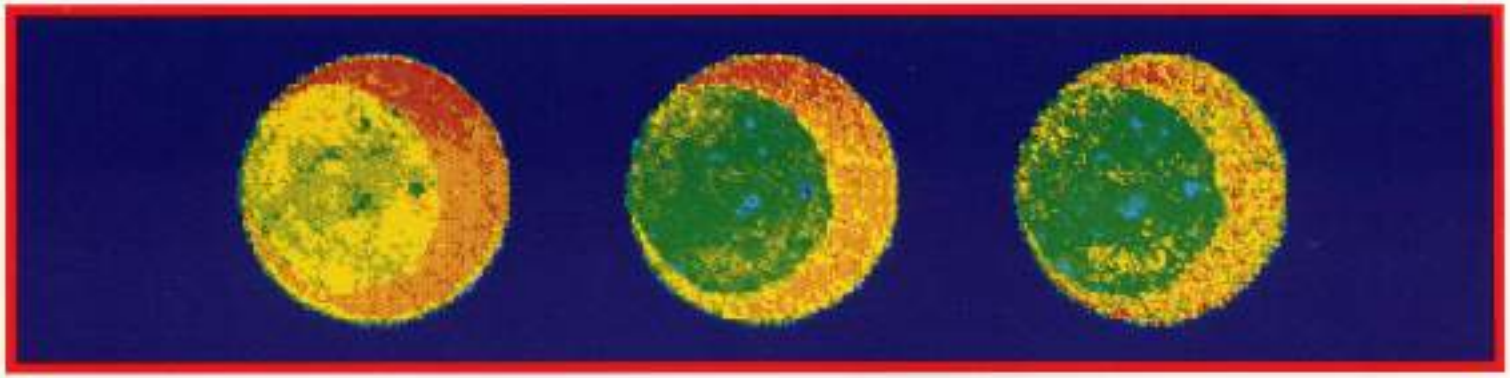

Dioxane proton image of highly crosslinked sulfur-vulcanized rubber. Sample swollen in dioxane

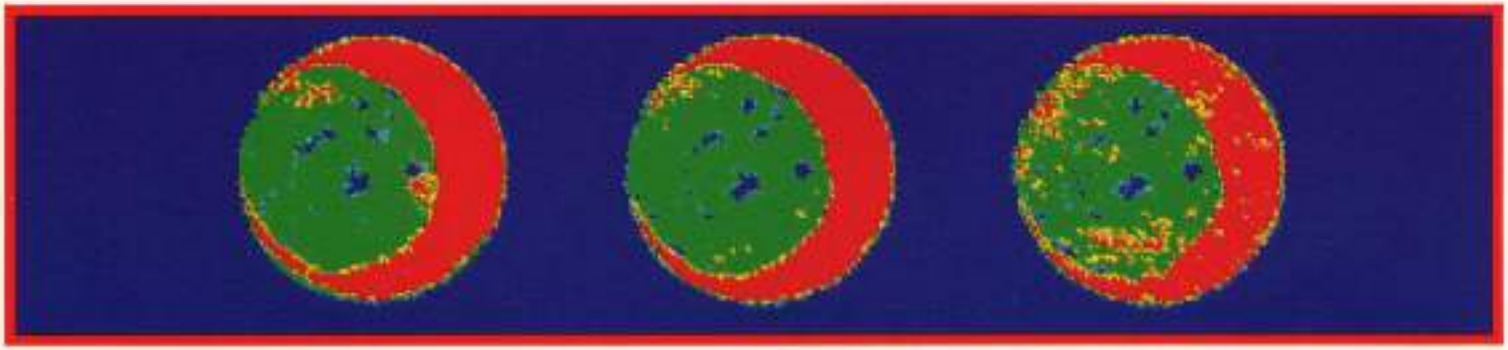

Contour plot of above image, showing regions of heterogeniety in rubber.

CONCLUSIONS

It is obvious that there is considerable inhomogeneity in the crosslinking for this rubber sample. Such inhomogeneities could arise from improper mixing, thermal gradients, or variations in the vulcanization chemistry.

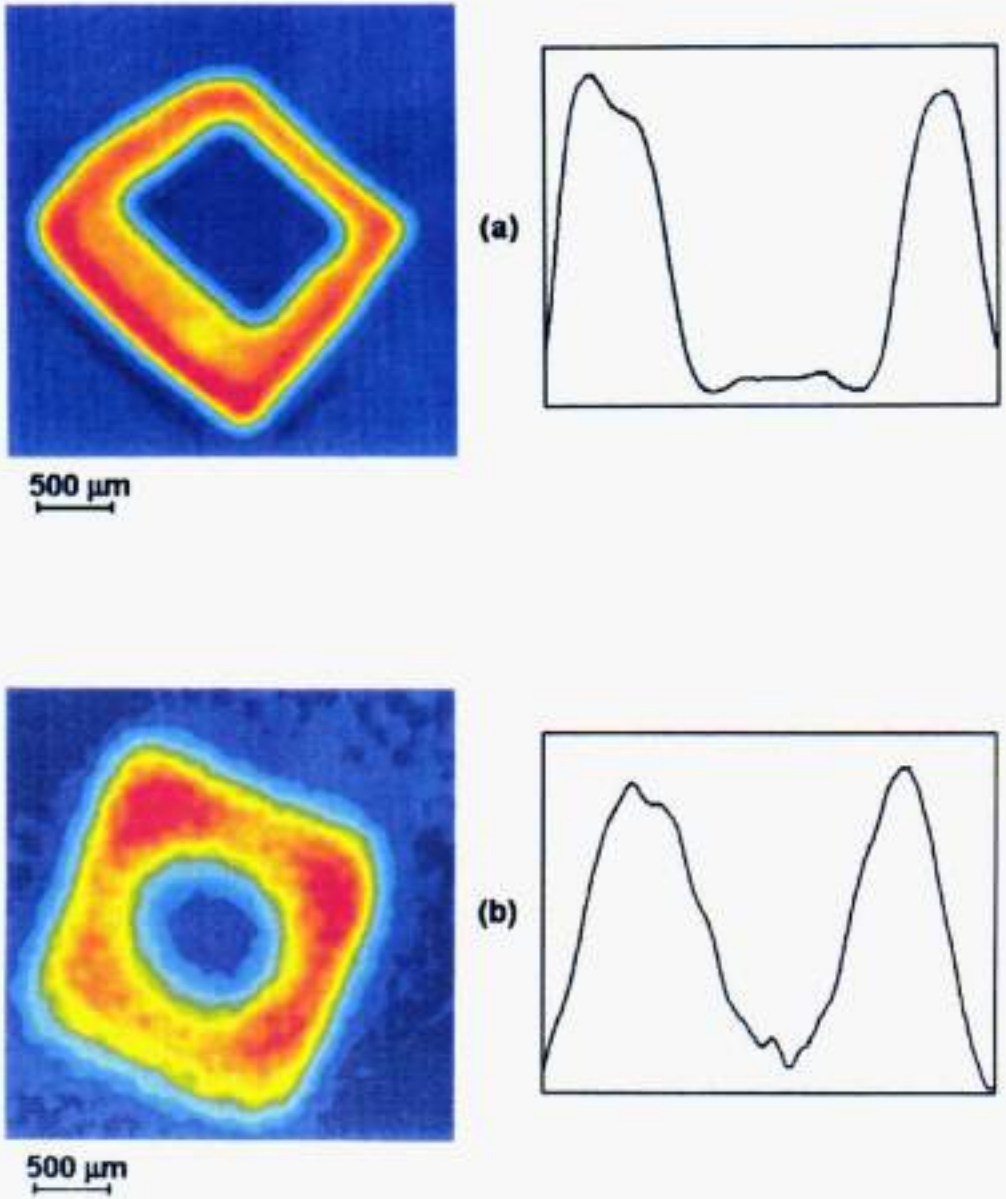

Figure 1. (a) Toluene in PVC and (b) *n*-pentane in PEhd. Left: two-dimensional images. The color goes from red (highest spin density) to dark blue (lowest spin density). Right: characteristic penetration profiles extracted from a cross-section through the corresponding image.

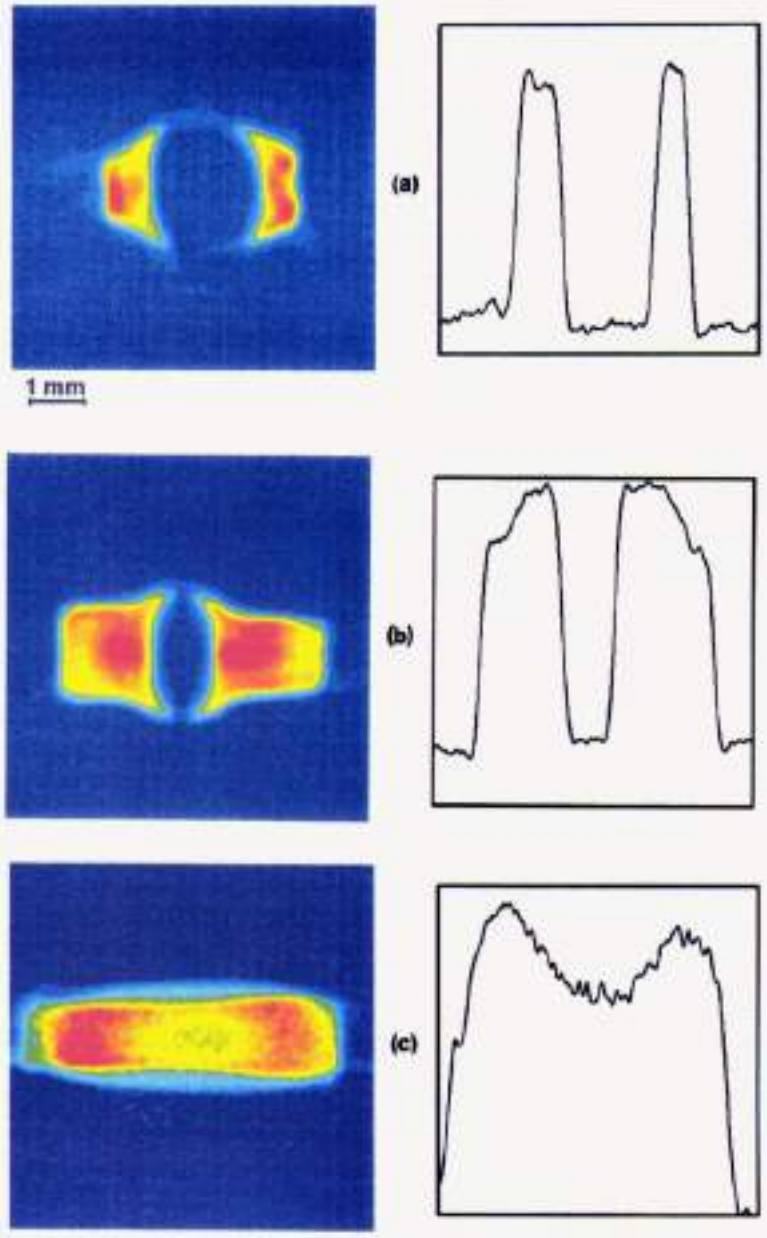

Figure 2. Solvent penetration in stretched PVC and swelling, after 14 h (a) and 30 h (b) of immersion in toluene, and final state after 30 h of immersion in trichloroethylene (c). Cross-sections (diffusion profiles) along the direction of preferential solvent penetration are shown on the right. The color scale is identical to the one for Figure 1.